Supplementary Figures

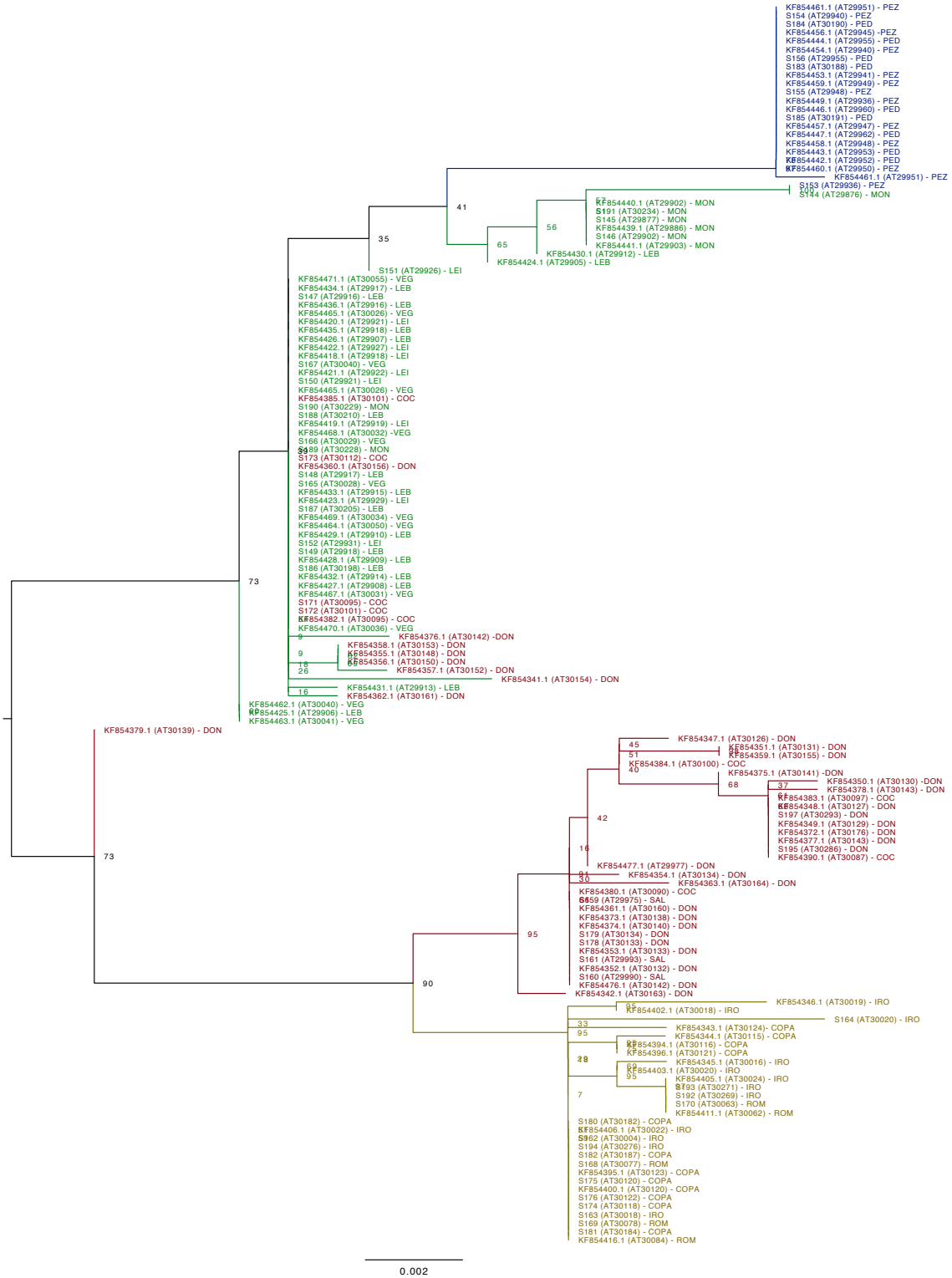

Supplementary Figure 1. Maximum-likelihood phylogeny based on the mitochondrial cytochrome b (MT-CYB) alignment including 50 sequences generated in this study and 96 additional records from González et al. (2014) obtained from GenBank (supp. Table 1). The tree was inferred with IQ-TREE under the best-fit substitution model selected by ModelFinder, with node support assessed using SH-aLRT and 1,000 ultrafast bootstrap replicates. Colours indicate the four major mitochondrial lineages recovered (Inland, Doñana coastal, Iro–Conil system, and Guadalete drainage). This topology is highly congruent with the complete mitogenomes (Fig. 3b) and the WGR trees (Fig. 3a), recovering the same four clades with minor differences in deeper branching patterns.

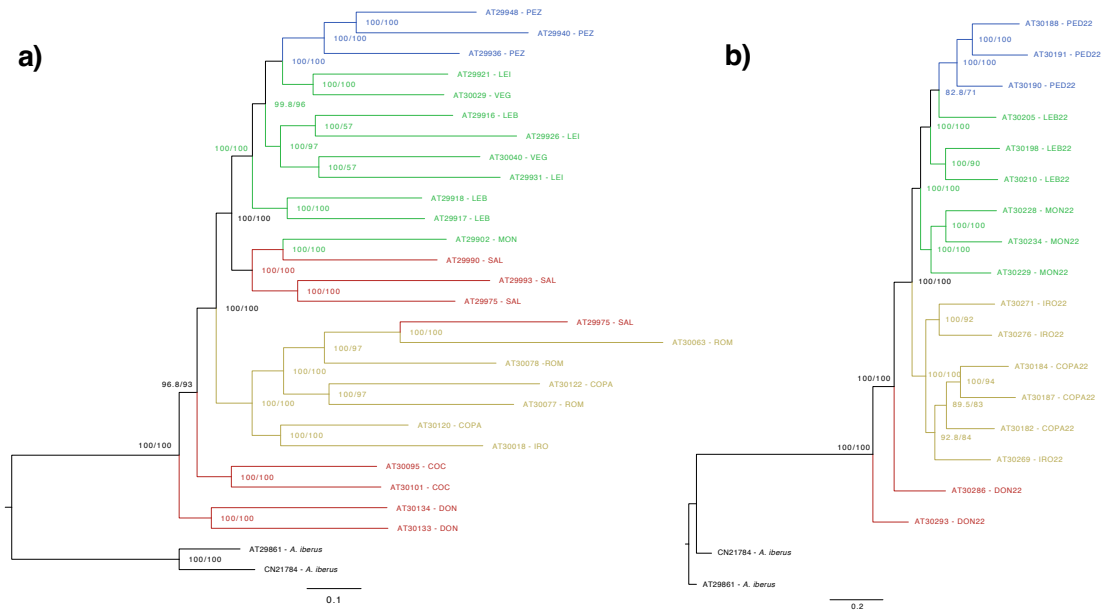

Supplementary Figure 2. *Maximum-likelihood phylogenies inferred from whole-genome SNP datasets for (a) the 2008 samples and (b) the 2022 samples. Trees were reconstructed in IQ-TREE under the best-fit substitution model selected by ModelFinder, with node support assessed using SH-aLRT and 1,000 ultrafast bootstrap replicates. Two Aphanius iberus individuals of comparable sequencing coverage were included as outgroups. Both temporal datasets recover the same four major genetic lineages (Inland, Doñana coastal, Iro–Conil system, and Guadalete drainage), showing highly consistent clustering across years despite increased differentiation in the 2022 dataset.*

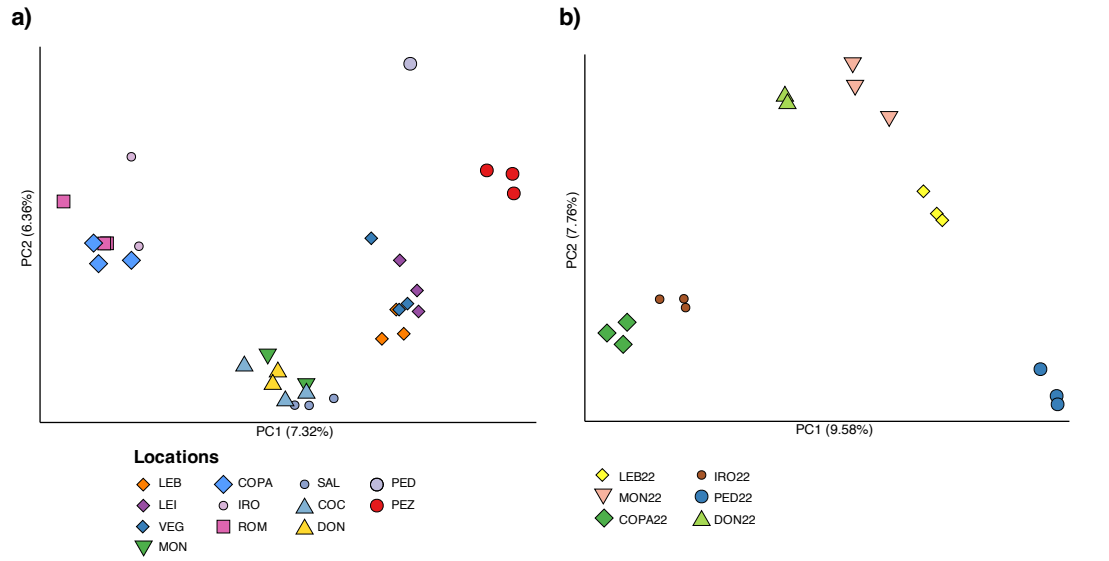

Supplementary Figure 3. Principal Component Analyses (PCA) of genome-wide SNP variation for (a) the 2008 dataset and (b) the 2022 dataset. Each point represents an individual, coloured and shaped according to its population of origin. Both temporal datasets recover the same four major genetic lineages (Inland, Doñana coastal, Iro–Conil system, and Guadalete drainage), with individuals from each population clustering consistently across years. The 2022 PCA shows increased inter-population separation relative to 2008, reflecting the rise in genetic differentiation documented in the temporal analyses,

Supplementary Tables

Supplementary Table 1. Cytochrome b (MT-CYB) sequences included in the haplotype network analysis. The table lists each sequence, assigned haplotype, genetic lineage, population of origin, internal sample code (AT ID), original GenBank identifier when applicable, accession number (GenBank or this study), NCBI GenBank accession number, and notes on duplicated sequences (yellow cells indicate haplotype discordances).

Supplementary Table 2. Model support statistics for ADMIXTURE and STRUCTURE clustering analyses of the "full strict" dataset. ADMIXTURE cross-validation (CV) error values are shown for K = 2–8, with the minimum CV at K = 2 indicating the strongest upper-level partition. STRUCTURE results report mean log-likelihood values (lnP(D)) and standard deviations across three independent replicates per K (K = 1–8). The absence of a monotonic increase in lnP(D) and elevated variance at higher K values suggest hierarchical structure and limited model convergence; therefore, final clustering interpretation was based on replicate stability and concordance with PCA and phylogenetic analyses.

K	ADMIXTURE CV	STRUCTURE mean lnP(D)	SD
2	0.40542	-5,251,838	7,530
3	0.45554	-5,385,364	10,627
4	0.51768	-5,603,726	322,336
5	0.59568	-5,952,684	298,979
6	0.66349	-5,727,842	354,520
7	0.75721	-8,299,238	1,503,425
8	0.82027	-6,178,827	42,634

Supplementary Table 3. Treemix model fit for the 2008 dataset across migration parameters (m = 1–12). For each value of m, the table reports the final log-likelihood of the model. Higher numbers of migration edges consistently increased model likelihood, with the best-supported models occurring at m ≥ 7, indicating a historically complex reticulation pattern among populations.

Migrations	Likelihood Final
12	545,67793
11	545,06046
10	542,91163
9	537,10147
8	536,5497
7	533,17308
6	524,65558
5	519,96734
4	512,10503
3	492,43838
2	479,79847
1	440,68066

Supplementary Table 4. Treemix model fit for the 2022 dataset across migration parameters (m = 1–6). Reported values correspond to the final log-likelihood of each model. Likelihoods plateau at m = 4–6, indicating that only a small number of migration edges is supported in 2022, consistent with a more tree-like, weakly connected population structure compared to 2008

Migrations	Likelihood Final
6	162,87474
5	162,87474
4	162,87458
3	162,84556
2	162,81616

1	162,72817

Supplementary Table 5. Pairwise absolute nucleotide divergence (Dxy) and relative genetic differentiation (Fst) among populations of Aphanius baeticus for 2008 calculated with pixy, using variant and invariant sites. Each row corresponds to a pairwise population comparison (Var1–Var2), with Dxy representing absolute divergence per site and Fst representing relative differentiation between populations. Values are ordered from highest to lowest Dxy/Fst to facilitate visualization of major genetic breaks among lineages.

Supplementary Table 6. Pairwise absolute nucleotide divergence (Dxy) and relative genetic differentiation (Fst) among populations of Aphanius baeticus for 2022, calculated with pixy using variant and invariant sites. Each row corresponds to a pairwise population comparison (Var1–Var2), with Dxy representing absolute divergence per site and Fst representing relative differentiation between populations. Values are ordered from highest to lowest Dxy/Fst to facilitate visualization of major genetic breaks among lineages

Var1	Var2	Dxy	Fst
PED22	COPA22	0.00206704866054198	0.291289759792102
LEB22	COPA22	0.00209304908755866	0.211719200977819
PED22	DON22	0.00226638032482375	0.20437702752519
PED22	IRO22	0.00206075403486991	0.198270565187934
MON22	COPA22	0.00215727391523385	0.188790762038674
DON22	COPA22	0.00224280348511269	0.173563633396391
PED22	MON22	0.00200490707158537	0.156436913148218
MON22	IRO22	0.00217956342724088	0.125310618543215
LEB22	IRO22	0.00207502789039529	0.121183638519729
LEB22	DON22	0.00228753867294032	0.120520461202095
IRO22	DON22	0.00230990340997982	0.111856995989725
PED22	LEB22	0.00174571589027404	0.102040893908549
MON22	DON22	0.00231473030083759	0.0959435867908873
MON22	LEB22	0.00200229174102933	0.073751046374739
IRO22	COPA22	0.00179401036604438	0.0480343623299464